PHYSICAL REVIEW B VOLUME 30, NUMBER 4 15 AUGUST 1984

Si(111) 7×7 reconstruction: Strain in the adatom model

Tsuyoshi Yamaguchi
Faculty of Engineering, Shizuoka University, Hamamatsu 432, Japan
(Received 6 December 1983; revised manuscript received 13 April 1984)

The adatom model of the Si(111) 7×7 structure obtained by scanning tunneling microscopy, which is an experiment in real space, is extended to take into account the displacement of atoms. The 12 first-layer adatoms in the unit cell have an sp^3-electron configuration; the 12 second-layer dangling-bond-site atoms have sp^2; the second-layer dangling-bond-site atom at the center of the half unit cell has $sp^{2.5}$. The adatoms shift upward by almost 50% of the layer distance. The dangling-bond-site atoms do not shift, and other second-layer atoms bonding with adatoms shift in the direction of the adatoms. The third-layer atoms shift by more than 25% of the layer distance. Changes in bond length are small and bond angles of surface-layer atoms change more than 10°; the strain energy is released by changing mainly bond angles. The atomic structure obtained gives quite revised spectra of ion scattering from the adatom model. The spectra are now close to those of the "pyramidal" model, which was previously asserted to be the best model explaining the result of another experiment in real space, ion scattering. Furthermore, a mechanism of the phase transition from the 7×7 structure to others by a coherent motion of adatoms is presented.

I. INTRODUCTION

The determination of the atomic structure of the reconstructed 7×7 structure of the Si(111) surface is one of the most challenging in the field of surface science. Many experimental and theoretical studies have been done; the number of models is a few tens and has been ever increasing. Here, the complexity of the large unit cell with 49 atoms in a layer makes the analysis of experimental work difficult: Models in accordance with one set of experiments are in conflict with others. Another reason for such chaotic status is that all earlier experiments were done in $\vec{k}$ space; experiments in $\vec{k}$ space inevitably have the ambiguity that the scattering center cannot be determined uniquely as an adatom, impurity, or vacancy.

We now have, however, two experiments in real space, namely scanning tunneling microscopy as performed by Binnig *et al.*[1] and ion-scattering spectroscopy as performed by Aono *et al.*[2] These two experiments and those of different types which will be done in real space in the future will settle the feverish competition surrounding the determination of the Si(111)7×7 structure.

The Binnig model[1] has 12 adatoms in the unit cell, leaving 13 dangling bonds in the second layer; the number of dangling electrons in this model is 25. An adatom is located at the site where no atom appears in the third layer (in this paper, the layer of adatoms is called the first layer). At the corner of the cell, there is no adatom. The atomic arrangement has mirror symmetry with respect to the long diagonal of the cell and threefold-rotational symmetry at the corner. We stress that there is no mirror symmetry with respect to the short diagonal of the cell. If we calculate the strain energy by the method described in Sec. II, we obtained a value of 77.39 eV per unit cell.

The experiment of Aono *et al.*[2] for low-energy He^+-ion scattering showed that if we see the surface in terms of ion scattering, the surface has approximate mirror symmetry with respect to the short diagonal of the unit cell, together with symmetry properties clarified by Binnig *et al.*[1] In their "pyramidal" model, three-membered rings of lower adatoms are located at the on-top site of the surface layer, and an upper adatom is located at the hollow site of the three-membered adatom rings. The positions of the pyramidal clusters are the same as the adatoms of Binnig *et al.*[1] Another characteristic of their result is that the spectrum at relatively low angle (10°–17°) with respect to the short diagonal has a strong intensity; this cannot be explained by the Binnig model, which has no atomic displacement. There is also no atomic displacement in the Aono model. We calculated the elastic energy of this model and found the structure without atomic displacement to be the energetically stable solution. However, as the number of dangling electrons is 97 [=13 + (12×7)], the surface energy of this model seems to be very high.

As mentioned earlier, there are many models in addition to the above two models (see references in Ref. 2). However, we take the Binnig model,[1] which seems to be the most plausible to us, and extend it to take into account the strain energy.

The surface structure which is realized has the lowest total energy, including the electronic energy between dangling electrons and the strain energy due to atomic displacement. In the Binnig model,[1] if one set of dangling electrons is converted to the other, the number of dangling electrons is only one. Then, the interaction between dangling electrons can be neglected because of the large unit cell. Furthermore, we neglect the polarization interaction between adatoms and dangling-bond-site atoms due to the conversion of the dangling electrons. We also neglect the adatom-adatom interaction. Thus, we minimize only the energy of displacement of the atoms, using the method of

 ©1984 The American Physical Society

Appelbaum and Hamann,[3] which takes into account the total interaction energy between two atoms (stretching interaction) and three atoms (bending interaction). As is shown later, the atomic arrangement obtained can give approximate mirror symmetry with respect to the short diagonal of the unit cell in the ion-scattering model.[2] As for the relatively strong intensity at low angles, with respect to the short diagonal, our modified Binnig model gives quite revised spectra from the original Binnig model. The new spectra resemble those of the Aono model; the latter was asserted to be the best model to explain the ion-scattering spectra. The strain energy of our model is 61.82 eV per unit cell.

Here, it should be noted that the model of Northrup and Cohen[4] of the Si(111)2×1 structure was obtained by converting a dangling electron of one atom in a unit cell to the other; the former atom has an sp^2-electron configuration and the latter atom has an sp^3-electron configuration. It is well known that atoms with sp^2- and sp^3-electron configurations combine with three and four atoms at the corners of the equilateral triangle in a plane and the tetrahedron in three dimensions, respectively. Then, the surface becomes flat in the region near the sp^2 atom and swollen near the sp^3 atoms.

II. MINIMIZATION OF STRAIN ENERGY

We restrict ourselves to finding the static equilibrium position of atoms in the Si(111)7×7 reconstructed structure. In such a classical limit the expression of elastic surface energy due to atomic displacement is the same as that of Appelbaum and Hamann,[3] who adapted Keating's model[5] for bulk Si crystal to the Si(100)2×1 surface,

$$E=\alpha \sum_{\substack{\text{all}\\ \text{bonds}}} (\vec{X}_{ij}^{\,2}-3a^2/8)^2+\beta \sum_{\substack{\text{all}\\ \text{bond}\\ \text{pairs}}} (\vec{X}_{ij}\cdot\vec{X}_{jk}+a^2/8)^2 , \tag{1}$$

if the crystal is of the diamond structure where each atom has an electron configuration sp^3. The first and second terms represent bond-stretching and bond-bending interactions between nearest-neighbor atoms, respectively. α and β denote the corresponding force constants. $\vec{X}_{ij}$ $(=\vec{X}_i-\vec{X}_j)$ is a relative atomic displacement and a $(=3.84$ Å$)$ is the lattice constant of the unreconstructed surface.

We first take the Binnig model.[1] If we change independently, in the minimization process for the energy (1), the positions of atoms in the first through seventh layers, the number of degrees of freedom becomes tremendously large, $[12+(49\times6)]\times3=918$. We make the following three assumptions.

First, the arrangement of atoms in the reconstructed structure has the same symmetry properties as the unreconstructed structure, namely mirror symmetry with respect to the long diagonal of the unit cell and threefold-rotational symmetry at the corner of the cell. This is similar to the assumption by Appelbaum and Hamann.[3] There are three inequivalent cells. Then, as shown in Fig. 1, our new "unit cell" is an equilateral triangle; the length

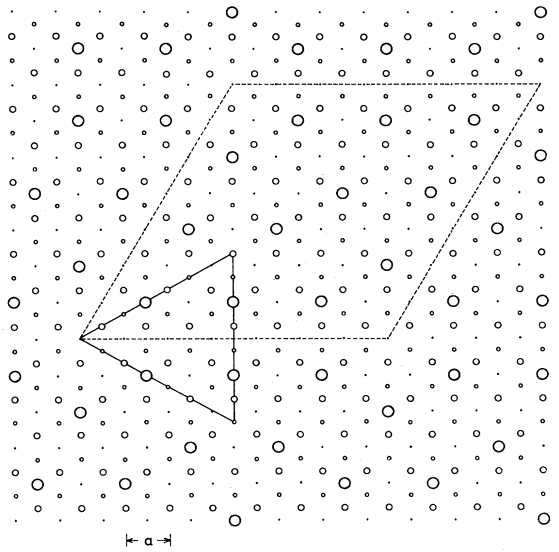

FIG. 1. 7×7 unit cell and three inequivalent mirror symmetries along the long diagonal of the unit cell represented by dashed and solid lines, respectively. The first-, second-, third-, and fifth-layer atoms are represented by circles with diameters which become smaller for deeper-layer atoms. The fourth-, sixth-, seventh-, and eighth-layer atoms are hidden behind the third-, fifth-, second-, and seventh-layer atoms, respectively. Note that there are also the fifth-layer atoms behind the first-layer adatoms. The equilateral triangle which has an area one-sixth of that of the unit cell and is bounded by the mirror-symmetry lines is our new "unit cell" in the calculation.

of edge is $7a/\sqrt{3}$. The area of our unit cell is one-sixth that of the real unit cell. Our unit cell has 76 atoms in the first through seventh layers. However, the mirror symmetry with respect to the edge of our cell reduces the number of degrees of freedom to 176.

Although the freedom is still pretty large, the expression for the energy which should be minimized is a biquadratic function of each relative displacement $\vec{X}_{ij}$. Then, the minimization is completed relatively easily. In reality, we obtain the same result, even if we change the initial values, the step sizes and the step signs of some of the parameters $\vec{X}_{ij}$.

Second, the ratio of force constants is fixed to that of the bulk, $\beta/\alpha=0.29$.[5] As is shown later, the relaxation of adatoms is large. Then, it is necessary to use many anharmonic terms higher than those of Keating model[5] for surface atoms. There is, however, no experimental or theoretical work from which we can obtain the interaction constants. Assuming that the relaxation decays exponentially for bulk atoms, we take the bond length (another parameter to be minimized) as

$$(\sqrt{3}a/2\sqrt{2})[1+b\exp(-z/z_0)] , \tag{2}$$

where z is the depth of the center of the bond from the surface, and b and z_0 are fitting parameters.

Our third assumption is the conversion of the dangling electrons between the dangling-bond-site-atoms (the second-layer atoms which are not combined with an adatom) and the adatoms (the first-layer atoms). The bending

interaction of atoms with the electron configuration sp^2 is written as

$$\sum_{\substack{\text{all}\\ \text{bond}\\ \text{pairs}}} (\vec{X}_{ij}\cdot\vec{X}_{jk}+3a^2/16)^2 \tag{3}$$

instead of the second term of Eq. (1). Here, as shown in Fig. 2, the mirror symmetry divides 12 adatoms in the real unit cell into four groups, each of which has three adatoms, and 13 dangling-bond-site atoms into four groups which have three, six, three, and one atoms, respectively. Then we assume that the atom with an $sp^{2.5}$ configuration is located at the center of the lower left half of the unit cell (the dangling-bond-site atom of the fourth group) and the bending interaction should be the average of types of Eqs. (1) and (3). We took the magnitude of converting dangling electrons between adatoms of the four groups, between dangling-bond-site atoms of the remaining three groups, and between adatoms and dangling-bond-site atoms as other parameters of the energy minimization. The calculation gives the result that all adatoms have an sp^3-electron configuration and all of the remaining dangling-bond-site atoms have an sp^2 configuration.

Since we give no energetic justification for transferring an electron from a dangling-bond-site atom to an adatom, there is no justification for using a modified Keating bond-bending term for these atoms. Furthermore, we have no available value of the ratio of force constants for graphitelike Si. We then assume that the ratio of force constants for atoms with an sp^2 configuration is also given by that of bulk atoms with an sp^3 configuration.

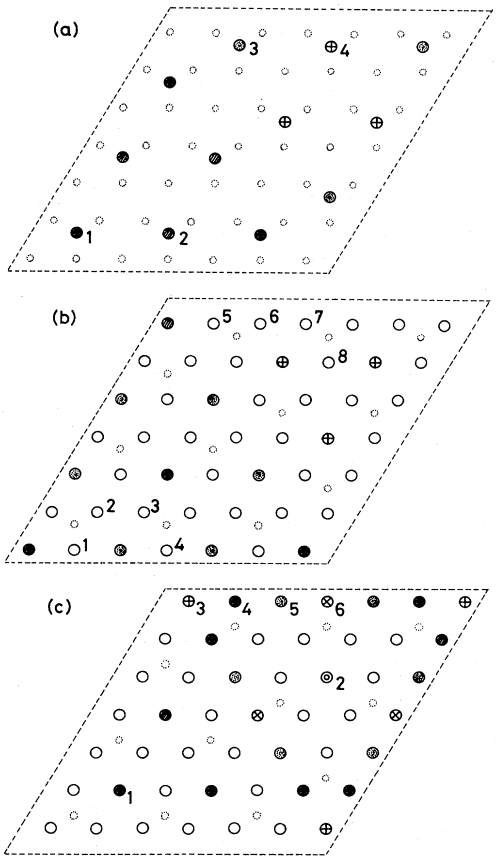

FIG. 2. Equivalent atoms of the first, second, and third layers. (a) Three equivalent adatoms of four groups represented by solid, shaded, hatched, and crossed circles. Dotted circle represents the second-layer atom. (b) Second-layer atoms. The solid circle represents the dangling-bond-site atom with the $sp^{2.5}$ configuration and the three shaded, six hatched, and three crossed circles represent three groups of dangling-bond-site atoms with sp^2 configuration. The open circles represent atoms with sp^3 bonding with adatoms: Numerals show six inequivalent atoms. One can easily find equivalent atoms by the mirror-symmetry argument. Dotted circle represents the first-layer adatom. (c) Third-layer atoms. These atoms are grouped into five by the nature of their bonding with the second-layer atoms, that is, atoms with numbers (1,2), 3, (4,6), 5, and others.

III. ARRANGEMENT OF ATOMS OF RECONSTRUCTED Si(111)7×7 STRUCTURE

First, let us discuss the physical origin of the reconstruction of the Binnig model[1] where 12 adatoms are adsorbed in order to lower the electronic interaction energy between 49 dangling electrons to that between 25 electrons. An adatom combines with three second-layer atoms: If the electron configuration of the adatom is sp^3 or sp^2, the preferable angle between the bond and the surface plane is 19.5° or 0°, respectively. However, the preferred angle for second-layer atoms is 90°. Although the angle between neighboring bonds of atoms with sp^3 or sp^2 configuration is 109.5° or 120°, respectively, there are two types of bending interactions between the first- (adatom), second- and third-layer atoms in the unreconstructed structure; the unit cell has 36 (=3×12) and 72 interacting bonds with angles of 180° and 70.5°, respectively. We then expect the reconstruction, which decreases the bond angle 180° and increases the bond angle 70.5° to angles nearer to 109.5° or 120°.

Second, the physical reasoning of the result that an adatom and a dangling-bond-site atom have the sp^3 and sp^2 configurations, respectively, comes naturally from the above discussion; the second-layer atom whose dangling bond before the adsorption of an adatom is normal to the surface plane prefers a bond angle of 19.5° to one of 0°.

Figures 3, 4, and 5, respectively, show the top and side

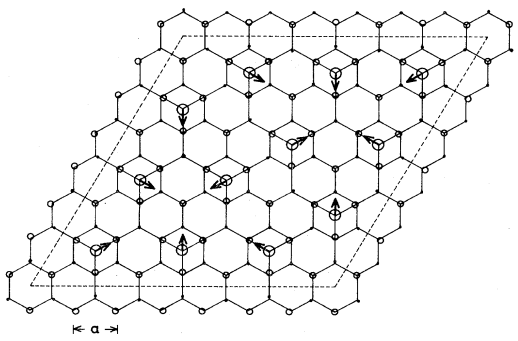

FIG. 3. Top view of atomic displacement of the first through third layers in the reconstructed structures represented by circles. The position of atoms of the unreconstructed structure is shown by the cusp of lines. An arrow shows the lateral direction of the shift of adatoms from the position in the unreconstructed structure, although it is not on the real scale.

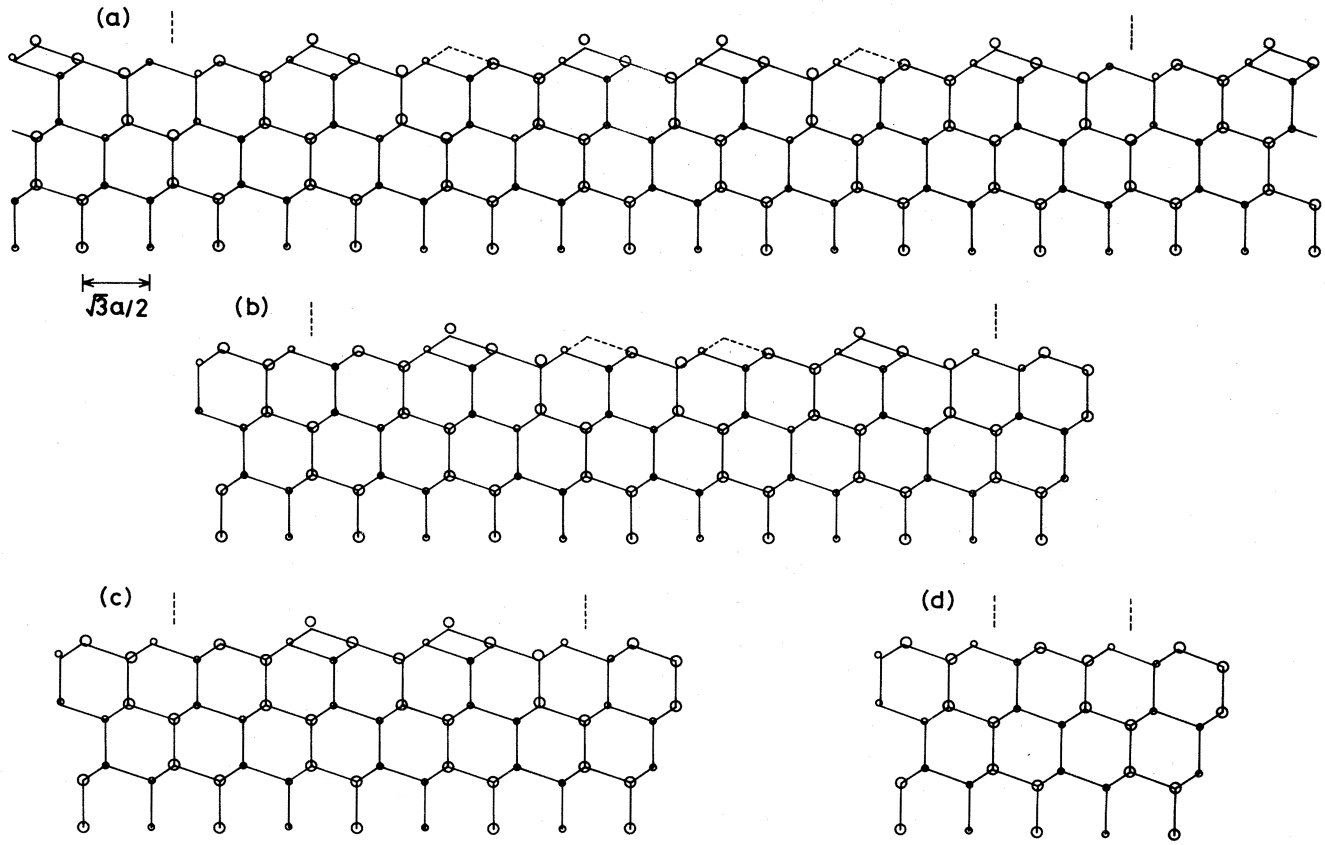

FIG. 4. Side view of the reconstructed structure parallel to the long diagonal of the unit cell. (a) First- and second-layer atoms represented by the large and small circles, respectively. Here, the first-layer atom is the atom on the long diagonal. (b) Third- and fourth-layer atoms. (c) Fifth- and sixth-layer atoms. (d) Seventh- and eighth-layer atoms.

views (parallel to short and long diagonals, respectively) of the reconstructed Si(111)7×7 structure.

The first-layer adatom with sp^3 configuration shifts almost upward from the position of the unrelaxed structure; the magnitude and the polar angle of the direction of displacement are given in Table I. Here, atoms of four inequivalent types are shown in Fig. 2(a). Note that these adatoms shift by more than 50% of the layer distance $a/2\sqrt{6}$. The upward shift results from bonding with three atoms of the second layer at symmetrical positions.

Values for the shift of adatoms in the case where bond lengths are not taken as independent parameters of minimization are, for comparison, given in Table I(b). The difference of shift between two cases is about 25%, although the difference of the minimized energies is only 1%. This indicates the importance of taking bond lengths as parameters of minimization.

Our calculation for both cases gives the result that the magnitude of the shift of adatoms perpendicular to the surface is the largest for adatom 1 (three adatoms in the inner region of the lower left half of the unit cell), next largest for adatom 3 (three adatoms in the inner region of the upper-right half of the cell), next smallest for adatom 2, and smallest for adatom 4. This is consistent with the observation that, as a whole, the contours of the scanning tunneling micrograph for one-half of the cell are higher than for the other half, if we consider that the observed contours for adatoms neighboring the hollow at the corner of the cell are apparently higher than those for others.

Atoms of the second layer are grouped into three categories, that is, 12 dangling-bond-site atoms, the dangling-bond-site atom at the center of the lower left half of the unit cell, and 36 atoms bonding with adatoms. Twelve atoms of the first category, which are, as mentioned earlier, further grouped into three by mirror symmetry with respect to the long diagonal, have the sp^2 configuration and do not shift at all within the accuracy of our calculation. In addition, the atom of the second category with $sp^{2.5}$ configuration does not shift. Thirty-six atoms of the third category with sp^3 configuration are pulled closer to the adatoms; the magnitude and the direction of displacement are given in Table II. This is due to the fact that the bond length of the reconstructed structure does not change so much from that of the unreconstructed one; the strain energy of the surface is released mainly by changing the bond angles, as will be shown below. This causes further displacement of atoms in deeper layers.

All atoms of the third layer have sp^3 configuration. Displacement of the third-layer atoms belongs to three categories, depending on the arrangement of neighboring second-layer atoms. First, four atoms at the center of the nearest three second-layer atoms bonding with adatoms shift almost upward; the magnitude and polar angle of the

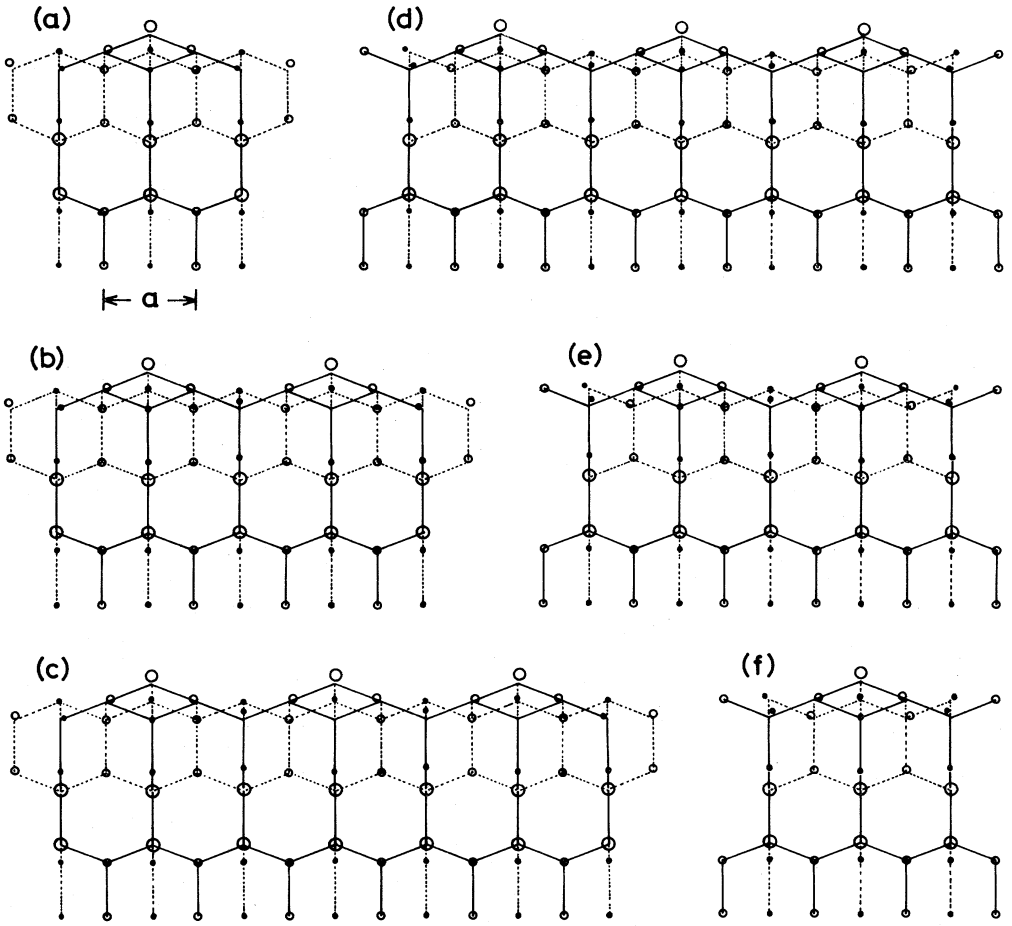

FIG. 5. Side view of the reconstructed structure parallel to the short diagonal. Large, medium, and small open circles represent atoms on the adatom layer, the nearest-neighbor layer, and next-nearest-neighbor layer, respectively. A solid line represents the bond between atoms on the adatom layer, the nearest-neighbor layer and the next-nearest-neighbor layer in the $[1\bar{2}1]$ direction. A dotted line represents a bond in the $[\bar{1}2\bar{1}]$ direction. (a) First-adatom layer along the long diagonal from the $[\bar{1}2\bar{1}]$ direction to $[1\bar{2}1]$. (b) Second-adatom layer. (c) Third-adatom layer. (d) Fourth-adatom layer. (e) Fifth-adatom layer. (f) Sixth-adatom layer.

TABLE I. Magnitude and direction of the shift of four inequivalent first-layer adatoms shown in Fig. 2(a). Absolute values of azimuthal angles [denoted by astersiks (*)] are fixed in the calculation. Azimuthal angles are for the numbered atoms in our unit cell shown in Fig. 2; values for other equivalent atoms are obtained via the symmetry argument. (a) The case where bond lengths are taken as independent parameters of minimization. (b) The case where bond lengths are not taken as independent parameters of minimization.

Atom	Magnitude	Polar angle (deg)	Azimuthal angle (deg)
		(a)	
1	0.095 79a	5.71	30.0*
2	0.102 49a	7.39	90.0*
3	0.092 59a	4.78	−30.0*
4	0.096 88a	4.39	−90.0*
		(b)	
1	0.128 61a	3.35	30.0*
2	0.135 45a	4.62	90.0*
3	0.127 19a	3.14	−30.0*
4	0.131 56a	3.12	−90.0*

displacement are given in Table III(a). Note that these atoms shift by about 40% of the layer distance. This upward shift is due to the fact that three neighboring second-layer atoms at symmetrical positions shift upward and outward. This upward shift is consistent, qualitative-

TABLE II. Magnitude and direction of the shift of eight inequivalent second-layer atoms which combine with adatoms. Inequivalent atoms are shown in Fig. 2(b). Note that the dangling-bond-site atom does not shift. Absolute values of azimuthal angles [denoted by asterisks (*)] are fixed in the calculation apart from their sign.

Atom	Magnitude	Polar angle (deg)	Azimuthal angle (deg)
1	0.064 63a	66.83	90.0
2	0.052 20a	57.63	−150.0*
3	0.055 75a	56.61	−28.2
4	0.072 03a	65.33	90.0*
5	0.064 24a	66.26	−30.0*
6	0.065 51a	62.30	−157.2
7	0.061 56a	61.67	−20.6
8	0.052 78a	58.72	90.0*

TABLE III. Magnitude and direction of the shift of six inequivalent third-layer atoms. Inequivalent atoms are shown in Fig. 2(c). Note that other third-layer atoms do not shift. (a) Third-layer atoms which shift almost upward. (b) Third-layer atoms which shift in a wavelike manner. Absolute values of azimuthal angles [denoted by asterisks (*)] are fixed in the calculation.

Atom	Magnitude	Polar angle (deg)	Azimuthal angle (deg)
		(a)	
1	0.093 17a	1.28	30.0*
2	0.084 51a	0.0*	0.0*
		(b)	
3	0.063 05a	41.59	−30.0*
4	0.054 27a	67.97	89.4
5	0.083 48a	30.16	−87.2
6	0.062 94a	68.40	90.0*

ly, with the characteristic feature the experimental result of Binnig *et al.* that the hollows with three arms in the lower left and upper right halves of the unit cell are both shallow. Second, the outermost 18 atoms in the upper right half of the unit cell shift in an alternate direction perpendicular to the line connecting these atoms: The magnitude of the shifts is larger than 25% of the layer distance, as given in Table III(b). These 18 atoms are divided into three groups: Three atoms of the first group, atom 3 in Table III(b), combine with two dangling-bond-site atoms and with a second-layer atom bonding with an adatom. Nine atoms of the second group, atoms 4 and 6, combine with two second-layer atoms bonding with an adatom and with a second-layer atom bonding with another adatom. Six atoms of the third group, atom 5, combine with two second-layer atoms bonding with different adatoms and with a dangling-bond-site atom. Third, the remaining 27 atoms do not shift: These atoms combine with two second-layer atoms bonding with an adatom and with a dangling-bond-site atom.

The lateral displacement parallel to the surface is calculated as follows. Although the maximum lateral displacement, 0.0655a (=0.251 Å), of one of the second-layer atoms is larger than 0.15 Å,[6] the average of lateral displacement of the first-, second-, and third-layer atoms is 0.0083a (=0.032 Å), 0.0349a (=0.134 Å), and 0.0169a (=0.065 Å), respectively. Then, our calculated result is consistent with the result of the high-energy-ion–scattering experiment,[2] namely that the lateral displacement of surface-layer atoms should be less than 0.15 Å.

Displacement of the fourth-layer atoms is similar to that of the third-layer atoms, although atoms of the third category shift slightly; it is within the range from 0.058 59a to 0.065 61a, from 0.020 37a to 0.058 59a, and from 0.004 29a to 0.006 68a for the first, second, and third categories, respectively.

Displacement of atoms of the fifth, sixth, and seventh layers becomes successively smaller; its magnitude ranges from 0.003 09a to 0.032 39a, 0.003 11a to 0.024 86a, and 0.004 03a to 0.006 99a, respectively.

The bond length of the reconstructed structure ranges, in units of the unreconstructed bond length $\sqrt{3}a/2\sqrt{2}$, from 0.9626 to 0.9693, 0.9725 to 1.0432, and 0.9898 to 1.0564 for the first-second–, second-third–, and third-fourth–layer atoms, respectively. The change in bond length for atoms of deeper layers is less than 1.5%. Here, values of parameters for the bond length b and z_0 in Eq. (2) are −0.042 73 and 0.184 15a, respectively. Note that the length of all bonds between the first- and second-layer atoms becomes shorter by about 4%, and the shortening of bond length disappears for the second-layer and deeper atoms. This conclusion that the surface shrinks remains the same, even if we fix all bond lengths to that of the bulk and minimize the energy ($b=0$).

Bond angles of the first-second-third–layer atoms which are 180° and 70.5° in the unreconstructed structure range from 164.1° to 168.0° and from 79.3° to 82.6°, respectively; the former decreases by more than 10° and the latter increases by about 10°. On the other hand, bond angles of the second-first-second–layer atoms change from 109.5° to values within the range from 97.9° to 101.7°; they decrease by about 10°. Changes in bond angle of deeper atoms from 109.5° have both positive and negative values. Their maximum absolute values decrease successively from 15.2° for the second-third-second–layer atoms to values less than 1° for the sixth-seventh-eighth–layer atoms. We note that even the bond angles of the seventh-sixth-seventh–layer atoms attain a maximum change of 1.6°.

IV. LOW-ENERGY ION SCATTERING

The low-energy ion-scattering spectroscopy of Aono *et al.*[2] is a powerful method for the structural analysis of surfaces in real space. In this spectroscopy, no incident ion can penetrate into the "shadow cone" of any surface atom; the shadow cone of a surface atom conceals other surface atoms depending on the ion incidence direction. The intensity of ion scattering increases stepwise as we change the ion incidence direction from the direction parallel to that normal to the surface. Here, the shape of the shadow cone is given well by the Thomas-Fermi-Moliere potential:[2] The fact that the diameter of the shadow cone is larger at a larger distance behind atoms gives the above result.

In quantitative comparison with experiment, one should take into account the ion neutralization; the scattering intensity by a deeper atom which is outside of the shadow cone of any surface atom decreases exponentially as a function of the depth from the surface. If we take the scattering intensity by an adatom as unity, the scattering intensity by second- and third-layer atoms with respective depths of $a/2\sqrt{6}$ and $a/\sqrt{6}$ in the unreconstructed structure is 0.460 and 0.212, respectively. Contributions from these atoms to the intensity become smaller in the reconstructed structure as follows: The intensities of a second-layer atom bonding with an adatom and a dangling-bond-site atom are about 0.320 and 0.283, respectively. The intensities of the third-layer atoms which shift almost upward, which shift in a wavelike manner, and which do not shift, are about 0.187, 0.172–0.140, and 0.130, respectively. Note that our definition of the depth dependence of the scattering intensity is slightly different from Aono *et al.*[2]

The calculated spectra are shown in Fig. 6 together with the experimental spectra. One can easily see that the spectrum of our model is quite revised from that of the Binnig model and close to that of the Aono model; the latter was asserted to be the best model to explain the result of the ion-scattering experiment.

The stepwise increase of the A spectrum at low angles of 3°, 4°, 5°, 7°, and 12° corresponds to the shadowing angles of two, two, two, three, and three adatoms by shadow cones of other adatoms which are at distances of $18a/\sqrt{3}$, $12a/\sqrt{3}$, $9a/\sqrt{3}$, $6a/\sqrt{3}$, and $3a/\sqrt{3}$, respectively, as given in Table IV(a). As the arrangement of adatoms is only mirror symmetric with respect to the short diagonal, we have the same spectra for the A and B spectra at low angles.

A criticism of the Binnig model[1] by Aono *et al.*[2] is that the A and B spectra of the former model are not similar to each other at high angles.

The stepwise increase of the B spectrum of the Binnig model at 26° corresponds to the shadowing angle of the atom by the shadow cone of the atom which is $a/2\sqrt{6}$ higher and at a lateral distance $2a/\sqrt{3}$, that is, the sum of the shadowing angle 15.1° at the lateral distance $2a/\sqrt{3}$ in Table IV and the tangential angle 10.0° $[=\tan^{-1}(1/4\sqrt{2})]$. The unit cell has 12 such second-layer atoms and 37 third-layer atoms, giving a large increase in intensity. Three and nine second-layer atoms among the above-mentioned 12 become visible in the reconstructed structure of our model at angles of 29° and 32°, respectively. Furthermore, three, one, seven, two, six, and eighteen third-layer atoms become visible successively at angles of 20°, 21°, 22°, 24°, 25°, and 27°, respectively. Note that the increase of intensity is much smaller than in the corresponding Binnig model due mainly to the large upward shift of the adatoms. Thus, the large abrupt intensity increase of the Binnig model at an angle of 26° is diminished to about two-thirds and the range is widened to the region from 20° to 32°, as shown by the interval between two arrows in Fig. 6(b). A similar discussion gives the spectra of Figs. 6(a) and 6(b). The A and B spectra of our modified Binnig model resemble each other: Our reconstructed surface seen by ion-scattering spectroscopy has approximate mirror symmetry with respect to the short diagonal of the unit cell.

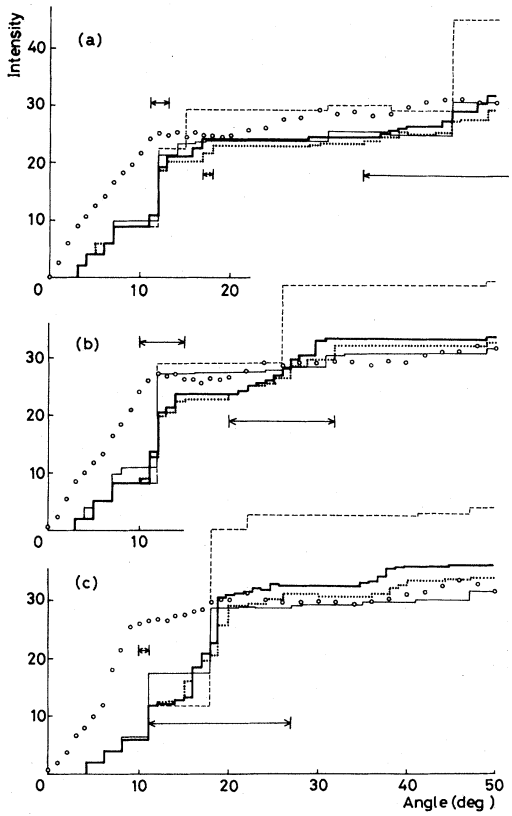

FIG. 6. Intensity of He^+-ion-scattering spectroscopy. The dashed, thin solid, and thick solid lines and the small circles show the spectra of the Binnig model, the Aono model, our model, and the experiment, respectively. The dotted line shows our spectrum where bond lengths are taken as independent parameters of the minimization of strain energy (see text). The experimental spectrum is normalized to the Aono model at 50°. Here, the angle of the ion direction of incidence is measured from the surface. The interval between two arrows shows the transition region in our modified Binnig model corresponding to a large abrupt increase of intensity in the original Binnig model. (a) A spectrum in the notation of Aono *et al.*; the azimuthal angle of the ion direction of incidence is along the $[\bar{1}2\bar{1}]$ direction of the long diagonal. (b) B spectrum; the azimuthal angle is along the $[1\bar{2}1]$ direction. (c) C spectrum; the azimuthal angle is along the short diagonal.

TABLE IV. Angles (in degrees) at which the shadow cone of a surface atom conceals atoms at various distances and at the same height for a He^+ ion of energy 0.93 keV. These angles are reflected in the stepwise increase of the intensity of the spectrum. (a) Shadowing angle for the ion incident along the long diagonal. For an approximate shadowing angle of a neighboring layer atom by the shadow cone of an atom, one should add the relative angle of those two atoms in the unreconstructed structure. (b) Shadowing angle for the ion incident along the short diagonal.

(a)	
$a/\sqrt{3}$	24.54
$2a/\sqrt{3}$	15.06
$3a/\sqrt{3}$	11.20
$4a/\sqrt{3}$	9.05
$5a/\sqrt{3}$	7.67
$6a/\sqrt{3}$	6.69
$7a/\sqrt{3}$	5.96
$8a/\sqrt{3}$	5.40
$9a/\sqrt{3}$	4.94
$10a/\sqrt{3}$	4.57
$12a/\sqrt{3}$	3.98
$18a/\sqrt{3}$	2.94
(b)	
a	16.7
$2a$	10.1
$3a$	7.4
$4a$	6.0
$5a$	5.1
$6a$	4.4
$7a$	4.0

The most crucial criticism of the Binnig model[1] by Aono *et al.*[2] is that the former cannot explain the strong intensity of the C spectrum at relatively low angles, 10°—17°, as the shadow cone of a surface atom conceals the atom at the distance a and at the same height up to about 18°: All the second-layer and deeper atoms of the Binnig model are invisible at angles below 18°, as shown in Fig. 6(c). We remind the reader of our calculated result that the dangling-bond-site atom does not shift in any direction and the second-layer atom at the distance a which combines with an adatom shifts by about $0.06a$: the tangential angle is about 4°. Then, the above-mentioned second-layer atom becomes visible at an angle of 14°. One should also note that the angle resolution of the ion-scattering spectroscopy used is a few degrees. Thus, our model gives the observed intensity at low angles along the short diagonal, although it is not completely satisfactory: The number of visible atoms at about 14° is the same as that of the Aono model[2] at above 18°. The discrepancy between the calculated and experimental spectra may be due to the difference of the definition of ion neutralization between theirs and ours, and may also be due to our approximations described in Sec. II.

For the case where bond lengths are not taken as independent parameters of the minimization of strain energy, we obtain the spectra shown by dotted lines in Fig. 6. As shown in Table I, the magnitude of shifts of adatom in this case is about 1.3 times that in the case where bond lengths are taken as independent parameters of the minimization. The ion-scattering intensity by deeper atoms in this case becomes smaller due to the exponential factor; we obtain the lower intensity at high angles, as shown in Fig. 6.

V. POSSIBLE 9×9-7×7-5×5-3×3 PHASE TRANSITIONS BY A COHERENT MOTION OF ADATOMS

As mentioned earlier, the 12 adatoms of the 7×7 structure are grouped into four shown in Fig. 2(a). In Fig. 3, an arrow represents the direction of the lateral shift of these adatoms in the reconstructed structure. The bonds between adatoms of the second and third groups and corresponding second-layer atoms are elongated and the other two bonds are shortened symmetrically. At high temperatures of about 800 °C, there is a possibility that the elongated bond is cut and the adatom moves to the on-top site of the third-layer atom, bonding with the dangling-bond-site atom ahead. As this site is energetically unstable, the adatom moves further to the site where there is no atom in the third layer; there are three such sites, the original and two ahead. If the adatom comes back to the original site, nothing occurs. However, there is a two-thirds probability of moving ahead and rebonding with a second-layer atom which originally bonds with another adatom. Then, the latter adatom which now has an energetically forbidden nearest-neighbor adatom moves to other nearest-neighbor-adatom sites. This process is repeated. If the route of subsequent adatoms becomes a closed loop, we have the 35×35 (approximate 5×5) structure of the adatom model. As it needs too much space to illustrate, we do not show the figure here.

By a similar motion of adatoms, we have the 5×5-3×3 phase transition, as shown in Fig. 7(a); strictly speaking, we have the 5×5-15×15 transition. Here, an arrow shows the motion of an adatom. The direction of the arrows of each loop can be reversed; here we show the case where the total angular momentum perpendicular to the surface does not vanish. If the adatoms represented by solid and dotted circles do not and do exist, respectively, we have the 3×3 structure. Starting from the 7×7 structure, we can obtain the 105×105 (approximately 3×3) structure via the 35×35 (5×5) structure and also the 21×21 (3×3) structure directly. Thus, we have a phase transition between any two of the $(2n+1)\times(2n+1)$ structures where $n=1,2,3,\ldots$.

The ratio of numbers of adatoms to the dangling-bond-site atoms is 0/1, 2/3, 6/7, 12/13, 20/21, and 30/31 for the 1×1, 3×3, 5×5, 7×7, 9×9, and 11×11 structures, respectively. Owing to the large gap of this ratio between the 1×1 and 3×3 structures, we cannot obtain the 3×3-1×1 phase transition by a similar motion of adatoms. The transition to the 1×1 structure at high temperature might be an order-disorder transition.

The closed loop of the 3×3-5×5-7×7-9×9-11×11 transition is an equilateral triangle on the whole. If the loop is a hexagon, we have the phase transition between

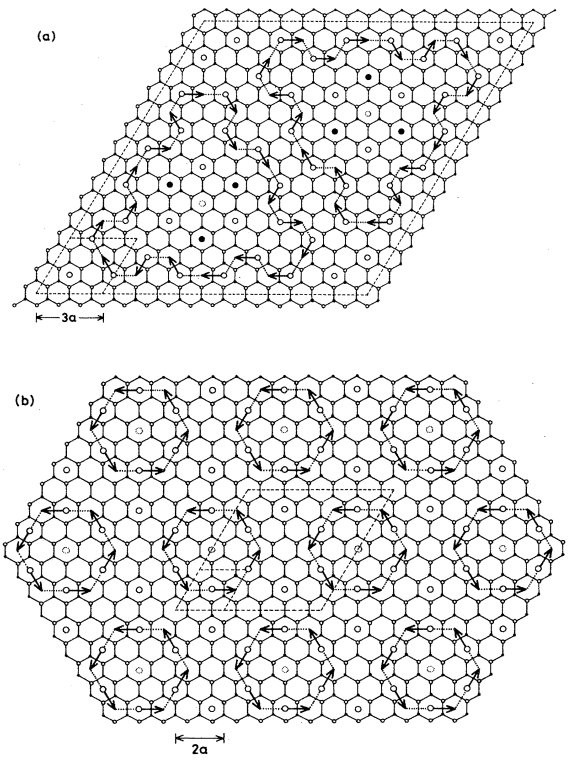

FIG. 7. Coherent motion of adatoms in a phase transition. Large open, medium open, and small solid circles represent the first-, second-, and third-layer atoms, respectively. (a) 5×5-15×15 (approximate 3×3) transition. The solid and dotted circles represent adatoms which do not and do exist in the 3×3 structure, respectively. (b) 3×3-6×6 (approximate 2×2) transition.

one of the 3×3, 5×5, 7×7, 9×9, and 11×11 structures and the 2×2 structure, as shown in Fig. 7(b). Note that the above ratio is 1/1 for the 2×2 structure.

The ratio is 1/0, 1/1, and 1/2 for the $\sqrt{3}\times\sqrt{3}$, $2\sqrt{3}\times2\sqrt{3}$, and $3\sqrt{3}\times3\sqrt{3}$ structures, respectively. Then, we can obtain the phase transition from the $m\times m$ structure to the $2\sqrt{3}\times2\sqrt{3}$ structure. However, as the loop becomes crossed in this case, this type of transition might not easily occur.

We have no information on the height and width of the potential barrier to the motion of an adatom; we simply point out the possibility of phase transitions from $m\times m$ structures to $mn\times mn$ (approximate $n\times n$) structures by a coherent motion of adatoms.

VI. DISCUSSION

The results in the preceding sections were obtained by assuming the same interaction constants α and β for all the bond-stretching and bond-bending energies as those in the bulk. It is well known that the interaction constants for the surface-layer atoms are usually quite different from those of the bulk. Taking interaction constants α and β of the type $\alpha=\alpha_0(1+\gamma e^{-\delta z})$ with parameters α_0, γ, and δ, and the depth from the surface z, we find a reconstructed structure which is qualitatively similar to that already described; quantitatively, we have a rougher or smoother surface according to the sign of parameter γ. In an extreme case where $\gamma=14.0$ and $\delta=2.0$, adatoms shift upward by 70—82 % of the layer distance. However, even such a rough surface does not give a better ion-scattering spectrum along the short diagonal, since the contribution from deeper ion becomes smaller due to the larger shift of adatoms.

ACKNOWLEDGMENTS

This work was done in collaboration with Professor S. Sugano of the Institute for Solid State Physics, University of Tokyo. The author thanks him for suggestions and discussion. Minimization of the free energy with respect to 176 and more variables was done by using the computer program, subroutine STEPIT (copyright 1965, J. P. Chandler, Physics Department, Indiana University); computation was performed at the Computer Center of the Institute of Molecular Science, Okazaki 444, Japan. This work was supported by a Grant-in-Aid for Special Project Research from the Ministry of Education, Science and Culture, Japan.

[1]G. Binnig, H. Rohrer, Ch. Gerber, and E. Weibel, Phys. Rev. Lett. **50**, 120 (1983).

[2]M. Aono, R. Souda, C. Oshima, and Y. Ishizawa, Phys. Rev. Lett. **51**, 801 (1983).

[3]J. A. Appelbaum and D. R. Hamann, Surf. Sci. **74**, 21 (1978).

[4]J. E. Northrup and M. L. Cohen, Phys. Rev. Lett. **49**, 1349 (1981).

[5]P. N. Keating, Phys. Rev. **145**, 637 (1966).

[6]R. J. Culbertson, L. C. Feldman, and P. J. Silverman, Phys. Rev. Lett. **45**, 2043 (1980).